

Design of Folic Acid-Conjugated Nanoparticles for Drug Targeting

BARBARA STELLA,^{1,2} SILVIA ARPICCO,² MARIA TERESA PERACCHIA,^{1*} DIDIER DESMAËLE,³ JOHAN HOEBEKE,⁴ MICHEL RENOIR,¹ JEAN D'ANGELO,³ LUIGI CATTEL,² PATRICK COUVREUR¹

¹ Université Paris-Sud XI, Physico-Chimie-Pharmacotechnie-Biopharmacie, UMR CNRS 8612-5, rue J. B. Clément, 92296 Châtenay-Malabry, France

² Dipartimento di Scienza e Tecnologia del Farmaco, 10125 Torino, Italy

³ URA CNRS 1843, Chimie Organique, 92296 Châtenay-Malabry, France

⁴ Université de Strasbourg, UPR CNRS 9021, I.B.M.C., 67084 Strasbourg, France

Received 17 March 2000; accepted 1 August 2000

ABSTRACT: The new concept developed in this study is the design of poly(ethylene glycol) (PEG)-coated biodegradable nanoparticles coupled to folic acid to target the folate-binding protein; this molecule is the soluble form of the folate receptor that is overexpressed on the surface of many tumoral cells. For this purpose, a novel copolymer, the poly[aminopoly(ethylene glycol)cyanoacrylate-co-hexadecyl cyanoacrylate] [poly(H₂NPEGCA-co-HDCA)] was synthesized and characterized. Then nanoparticles were prepared by nanoprecipitation of the obtained copolymer, and their size, zeta potential, and surface hydrophobicity were investigated. Nanoparticles were then conjugated to the activated folic acid via PEG terminal amino groups and purified from unreacted products. Finally, the specific interaction between the conjugate folate-nanoparticles and the folate-binding protein was evaluated by surface plasmon resonance. This analysis confirmed a specific binding of the folate-nanoparticles to the folate-binding protein. This interaction did not occur with nonconjugated nanoparticles used as control. Thus, folate-linked nanoparticles represent a potential new drug carrier for tumor cell-selective targeting. © 2000 Wiley-Liss, Inc. and the American Pharmaceutical Association *J Pharm Sci* 89: 1452–1464, 2000

Keywords: poly(ethylene glycol); poly(cyanoacrylate); nanoparticles; folic acid; surface plasmon resonance

INTRODUCTION

This paper proposes a new colloidal drug carrier obtained by chemical coupling of folic acid at its surface. Colloidal drug delivery systems for intravenous administration, such as liposomes and nanoparticles, represent a very attractive ap-

proach to achieve controlled release, prevent drug degradation, and avoid toxic effects. However, efficient drug delivery with these systems may be compromised by two factors: a short blood half-life (rapid elimination from the blood stream) and nonspecific targeting.

The rapid elimination from the blood stream is due to the recognition by the macrophages of the mononuclear phagocyte system (MPS) as a consequence of the adsorption of blood proteins (opsonins) onto the surface of colloidal carriers. This fact causes the accumulation of particulate drug carrier in the MPS organs, such as the liver and

Correspondence to: P. Couvreur (Telephone: 33-1-46-83-53-96; Fax: 33-1-46-61-93-34; E-mail: patrick.couvreur@cep.u-psud.fr)

Present address: Aventis, 94403 Vitry sur Seine, France

Journal of Pharmaceutical Sciences, Vol. 89, 1452–1464 (2000)
© 2000 Wiley-Liss, Inc. and the American Pharmaceutical Association

the spleen.¹ To obtain long-circulating colloidal drug carriers, it is possible to modify their surface with hydrophilic, flexible, and nonionic polymers, such as poly(ethylene glycol) (PEG).²⁻⁴

To solve the problem of site-specific targeting, some authors have attempted to increase the tissue specificity of colloidal drug carriers by coupling targeting agents, such as monoclonal antibodies.⁵⁻⁸ However, this approach has at least two drawbacks: the overall dimensions of the antibodies, which cause particles to diffuse poorly through biological barriers, and their immunogenicity. A way to solve these problems is to use small nonantigenic ligands. However, to our knowledge, no attempts have been made in coupling nanoparticles to small ligands for tumor targeting. Among the possible low molecular weight (MW) targeting agents, folic acid (MW = 441 Da) could be exploited to actively target cancer cells. Indeed, folic acid is a vitamin whose receptor is frequently overexpressed on the surface of human cancer cells.^{9,10} Therefore, this receptor has been identified as a tumor marker, especially in ovarian carcinomas,¹¹⁻¹³ although it is highly restricted in most normal tissues. In addition, the folate receptor is efficiently cell internalized after binding with its ligand (folic acid).^{14,15} Thus, folic acid presents advantages as a targeting agent. First, it is stable, inexpensive, and non-immunogenic compared with proteins such as monoclonal antibodies, as already explained. Second, folic acid has a very high affinity for its cell-surface receptor ($K_d \sim 1$ nM)¹⁴ and it moves into the cell cytoplasm,¹⁶⁻¹⁹ which is an advantage for more efficient intracellular delivery of anticancer agents than using a cell membrane marker that is not cell internalized.

Thus, the new concept proposed in this study is to design PEG-coated biodegradable nanoparticles conjugated to folic acid for the specific recognition of the soluble form of the folate receptor expressed at the surface of cancer cells. Here we describe the synthesis of the poly[aminopoly(ethylene glycol)cyanoacrylate-*co*-hexadecyl cyanoacrylate] [poly(H₂NPEGCA-*co*-HDCA)] copolymer, the preparation of the nanoparticles using that polymer, their characterization, the reaction of conjugation to folic acid, and the purification of the conjugate. Furthermore, to evaluate the ability of folic acid to address nanoparticles towards the soluble form of the folate receptor (also called folate-binding protein, FBP), we used surface plasmon resonance (SPR) technology, allow-

ing real-time analysis of the molecular association.²⁰

EXPERIMENTAL SECTION

Materials

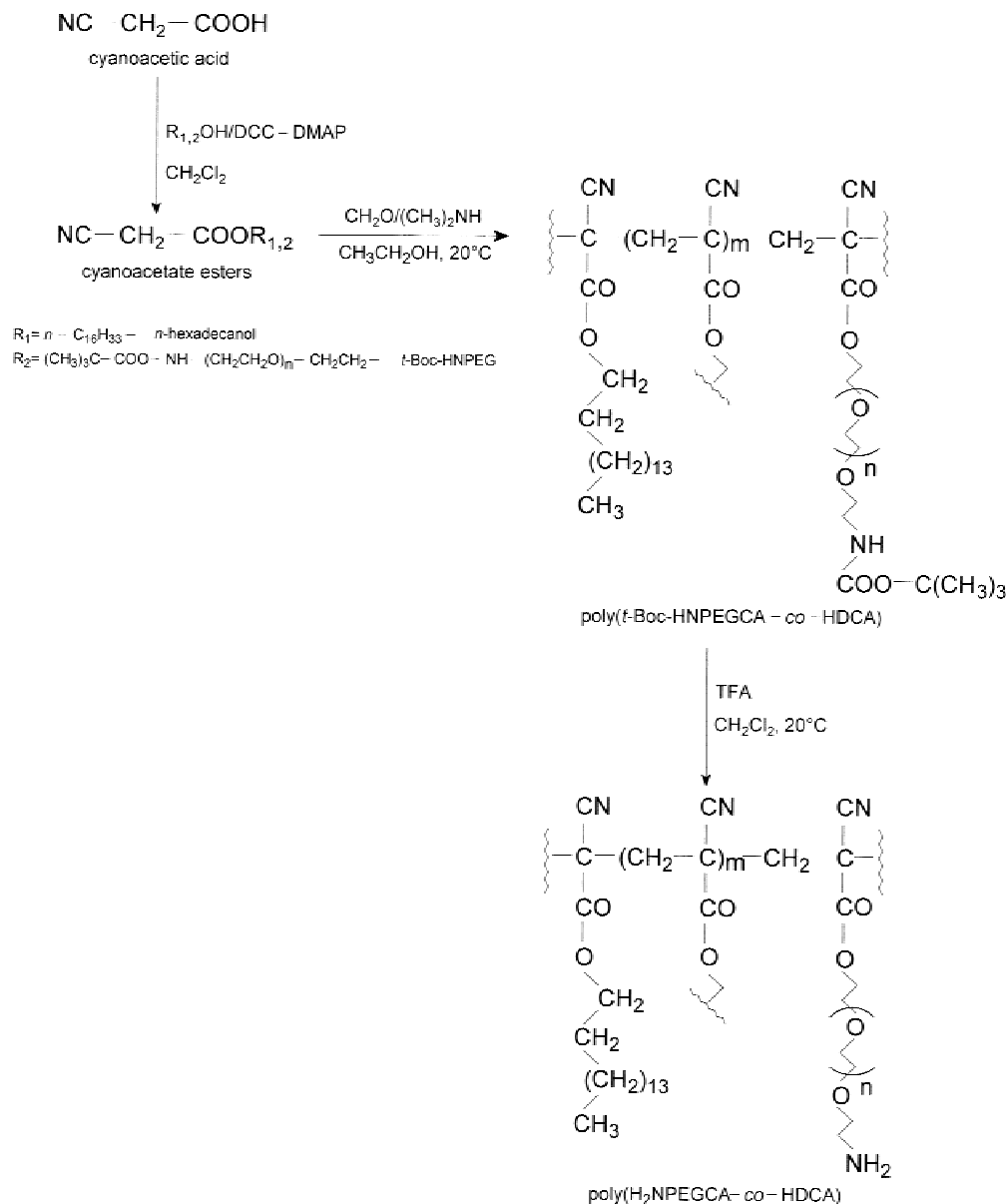
t-Boc-HNPEG 3400 was purchased from Shearwater Polymers, Inc. (Huntsville, AL). Cyanoacetic acid (purity, 99%) was obtained by Fluka (Buchs, Switzerland). *n*-Hexadecanol, trifluoroacetic acid (TFA), folic acid, and FBP were purchased from Sigma (St. Quentin, France). All other reagents were of analytical grade.

Synthesis of the Poly(H₂NPEGCA-*co*-HDCA) Copolymer

The cyanoacetate esters of *n*-hexadecanol and of *N*-(*tert*-butyloxycarbonyl)aminopoly(ethylene glycol) (*t*-Boc-HNPEG) 3400 were prepared according to the method of Peracchia,³ with minor modifications (Scheme 1). Briefly, for the synthesis of the *n*-hexadecyl cyanoacetate (HDCA), *n*-hexadecanol (1.0 g, 4.1 mmol) was dissolved in 25 mL of dichloromethane and mixed with cyanoacetic acid (0.38 g, 4.5 mmol) in 2.5 mL of ethyl acetate. Then, 1,4-(dimethylamino)pyridine (DMAP; catalytic amount) dissolved in dichloromethane was added. The reaction mixture was cooled at 4 °C, and 1,3-dicyclohexylcarbodiimide (DCC; 0.93 g, 4.5 mmol) in dichloromethane was added in a dropwise manner. After stirring at room temperature under nitrogen for 6 h, hexane was added and the white solid that formed was filtered off. The mixture was concentrated and purified by flash chromatography (silica gel 60, 230–400 mesh, Merck, Darmstadt, D) eluting with hexan acetate (90:10). The ester was obtained as a white solid; yield: 1.2 g, 96% mp 51 °C; proton nuclear magnetic resonance (¹H NMR; CDCl₃, δ): 4.20 (t, 2H, COOCH₂), 3.46 (s, 2H, CNCH₂), 1.68 (m, 2H, OCH₂CH₂), 1.26 (s, 26H, CH₂), 0.88 (t, 3H, CH₃); electron-impact mass spectroscopy (EIMS; relative intensity) *m/z*: 309 (M⁺, 9), 294 (7), 280 (46), 266 (54), 111 (50), 97 (84), 84 (82), 69 (100), 55 (83), 43 (74).

For the synthesis of *t*-Boc-HNPEG 3400 cyanoacetate, the same procedure of Peracchia³ was followed, except that *N*-ethyl-*N'*-(dimethylamino)propyl)-carbodiimide (EDC) was used instead of DCC; yield: 89%.

The poly[*N*-(*tert*-butyloxycarbonyl)aminopoly(ethylene glycol)cyanoacrylate-*co*-hexadecyl cya-



Scheme 1. Synthesis of the poly(H₂NPEGCA-co-HDCA) copolymer.

noacrylate] [poly(*t*-Boc-HNPEGCA-co-HDCA)] copolymer was synthesized by condensation of *t*-Boc-HNPEG 3400 cyanoacetate with *n*-hexadecyl cyanoacetate (molar ratio, 1:5) in ethanol in the presence of formalin and dimethylamine, as previously described for the poly[methoxypoly(ethylene glycol)cyanoacrylate-co-hexadecyl cyanoacrylate] [poly(MePEGCA-co-HDCA)]³ and as shown in Scheme 1; yield: 84%.

Then, the amino group of *t*-Boc-HNPEG was deprotected by TFA in dichloromethane²¹ (Scheme 1): TFA (0.6 mL) was added to the co-

polymer (300 mg, 0.06 mmol) dissolved in dry dichloromethane (15 mL), and the reaction was carried out for 1 h at room temperature under magnetic stirring. The reaction mixture was then neutralized with 10% aqueous sodium bicarbonate solution and extracted with dichloromethane. The organic layer was dried over MgSO₄ and evaporated under reduced pressure to give a pale yellow waxy material.

The poly(hexadecyl cyanoacrylate) (PHDCA) and the poly(MePEGCA-co-HDCA) polymers were also synthesized as described elsewhere.³

Characterization of the Poly(H₂NPEGCA-co-HDCA) Copolymer

The poly(H₂NPEGCA-co-HDCA) copolymer structure was confirmed by NMR. The ¹H and ¹³C NMR spectra were recorded in CDCl₃ on a Bruker AC 200P, 200 MHz spectrometer, with tetramethylsilane as internal standard.

The MW of the poly(H₂NPEGCA-co-HDCA) copolymer was measured by gel permeation chromatography (GPC). The analysis was performed in tetrahydrofuran (THF) with a Waters liquid chromatograph equipped with a Waters 501 pump, 712 WISP, 745 data module, and R401 differential refractometer. Polystyrene (Polysciences, Inc., Warrington, PA) was used as the standard.

Preparation and Characterization of the Nanoparticles

Nanoparticles were prepared by nanoprecipitation.²² Practically, 20 mg of the polymer [PHDCA, poly(MePEGCA-co-HDCA), or poly(H₂NPEGCA-co-HDCA)] was dissolved in 4 mL of warm acetone, and this solution was added, with magnetic stirring, to 8 mL of MilliQ water. Precipitation of particles occurred spontaneously. After solvent evaporation under reduced pressure, an aqueous suspension of nanoparticles (2.5 mg/mL) was obtained. The particles were then filtered through a 1.2- μ m filter (Millex[®] AP, Millipore, St. Quentin, France) and stored at 4 °C.

The size of the nanoparticles was determined at 20 °C by quasi-elastic light scattering (QELS) with a nanosizer (Coulter[®] N4MD, Coulter Electronics, Inc., Hialeah, FL). The selected angle was 90°, and the measurement was made after dilution of the nanoparticles suspension in MilliQ water. The surface charge of the nanoparticles was evaluated by zeta potential measurements in water and in 0.01 M phosphate buffer at pHs ranging from 6.0 to 8.0 (Zetasizer 4, with a multi-8 correlator 7032, Malvern Inst., Malvern, UK). Surface hydrophobicity of the nanoparticles was also investigated by hydrophobic interaction chromatography (HIC). This analysis was performed with 1 mL of a nanoparticles suspension, which was injected into a column (bed volume, 10 mL) filled with propyl agarose. Nanoparticles were eluted with phosphate buffer saline (PBS, 53 mM sodium phosphate, 82 mM NaCl). Particles that interacted with the gel were removed by washing with PBS containing Triton[®] X-100 (0.1% w/v).

The optical density of the eluted samples was determined at 350 nm with a Beckman spectrophotometer (Beckman Inst., Fullerton, CA). The concentration of the nanoparticles in the suspension was based on dry weight analysis.

Preparation and Purification of Folate-Poly(H₂NPEGCA-co-HDCA) Nanoparticles Conjugate

Nanoparticles of poly(H₂NPEGCA-co-HDCA) were then conjugated to the folic acid, as shown in Scheme 2. For this purpose, the *N*-hydroxysuccinimide ester of folic acid (NHS-folate) was prepared by esterification of folic acid with *N*-hydroxysuccinimide (NHS) in dry dimethylsulfoxide (DMSO) in the presence of DCC and triethylamine as catalyst, as reported elsewhere;¹⁷ the structure of NHS-folate was confirmed by ¹H and ¹³C NMR spectra.

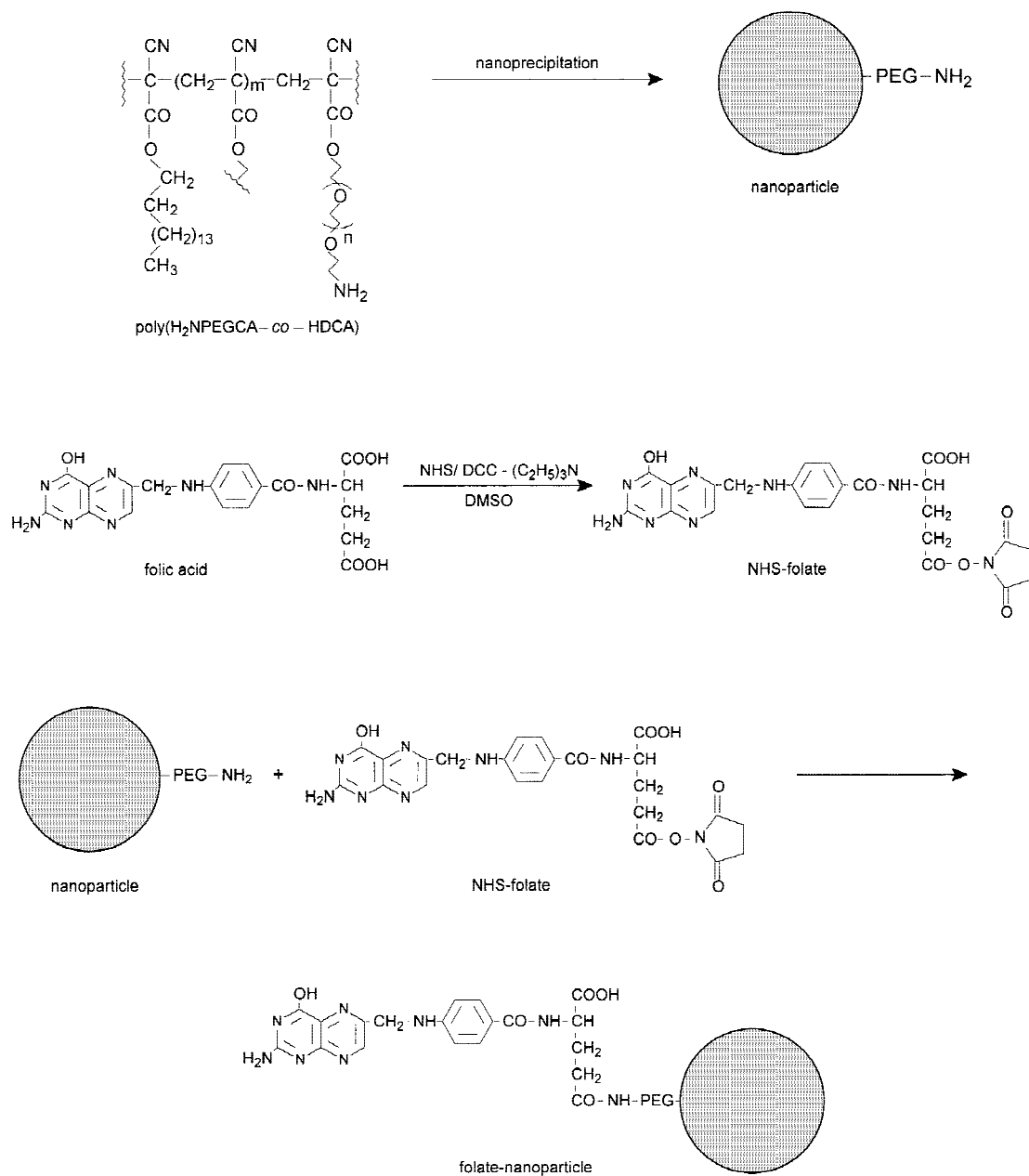
Then, NHS-folate (23 mg) was dissolved in DMSO (0.4 mL) and added to the nanoparticles suspension (4 mL, 5 mg/mL, pH adjusted to 9.0 with 5 mM carbonate/bicarbonate buffer, pH 11.5). The reaction was carried out for 30 min at room temperature.

To separate the folate-conjugated nanoparticles from unreacted folic acid and other byproducts, the reaction mixture was purified with a 3 × 14 cm Sepharose CL-4B column (Pharmacia Biotech., St. Quentin, France) using 5 mM carbonate/bicarbonate buffer, pH 9.0, as eluent. The optical density of the different collected fractions was monitored at 365 nm. The folate-nanoparticles, which eluted in the void volume, were then dialyzed against bicarbonate buffer and MilliQ water at 4 °C (Spectra/Por[®] 3500 MWCO dialysis membrane, Spectrum., Houston, TX).

The size of folate-nanoparticles conjugate was determined at 20 °C by QELS, with a nanosizer, as already detailed, and the stability of the formulation was evaluated by measuring the size of the particles after 1 month of storage at 4 °C in MilliQ water. Surface hydrophobicity of the folate-conjugated nanoparticles was investigated by HIC, with a propyl agarose column, as already described for the poly(H₂NPEGCA-co-HDCA) nanoparticles before folic acid conjugation.

Determination of Folate Content

The extent of folate conjugation on the folate-conjugated poly(H₂NPEGCA-co-HDCA) nanoparticles was determined by quantitative ultraviolet



Scheme 2. Preparation of the nanoparticles and conjugation with folic acid.

(UV) spectrophotometric analysis of the lyophilized product. The analysis was performed in DMSO/CH₂Cl₂ (4:1), and the amount of folic acid in the conjugate was evaluated by measuring the absorbance of the product at 358 nm (folic acid $\epsilon = 15,760 \text{ M}^{-1} \text{ cm}^{-1}$).

Surface Plasmon Resonance Measurements

To study the interaction of folic acid-conjugated poly(H₂NPEGCA-co-HDCA) nanoparticles with

the FBP, surface plasmon resonance measurements were performed with the upgraded BI-Acore 1000 (Pharmacia Biosensor AB, Uppsala, Sweden). Nonconjugated poly(H₂NPEGCA-co-HDCA) nanoparticles were used as control.

For this purpose, FBP was immobilized on the sensor surface of a carboxylated, activated, dextran-coated gold film, according to the general procedure for immobilization by amine coupling recommended by the BIAcore constructor.^{23,24} Briefly, after equilibration of the instrument with

HBS buffer (10 mM Hepes, 150 mM NaCl, 0.05% surfactant P20, pH 7.4), the following samples were automatically and successively injected into the BIAcore: (i) NHS/EDC in a mixed solution (1:1, v/v) to activate the carboxylated dextran; (ii) FBP dissolved at a concentration of 100 $\mu\text{g}/\text{mL}$ in 100 mM potassium phosphate buffer, pH 7.0, supplemented with 4 mM mercaptoethanol and 10% (v/v) glycerol; and (iii) 1 M ethanolamine in water, pH 8.5, to deactivate residual NHS-esters on the sensor chip. The immobilization protocol, which was performed at a flow rate of 2 $\mu\text{L}/\text{min}$, allowed the binding of 4 ng/mm^2 of FBP per channel.

The binding of poly($\text{H}_2\text{NPEGCA-co-HDCA}$) nanoparticles (both nonconjugated and folate-conjugated ones) to the sensorchip was performed at a flow rate of 5 $\mu\text{L}/\text{min}$ with a concentration of 5 mg/mL . The nanoparticles were allowed to interact with the FBP for 10 min. In view of the poor regeneration of FBP in 3 M KSCN, every nanoparticles suspension was tested on newly immobilized FBP. KSCN-denatured FBP was used as a control experiment where binding properties of folate receptor are lost.

In a second series of experiments, FBP was immobilized at 6 ng/mm^2 and 2.5 mg/mL of control particles, and folate-conjugated nanoparticles were allowed to interact at 5 $\mu\text{L}/\text{min}$ to study the kinetic parameters of the interaction. Under similar conditions, using a concentration of 1 mM folate, the kinetic parameters of the free folic acid were also determined.

RESULTS

Synthesis of the Poly($\text{H}_2\text{NPEGCA-co-HDCA}$) Copolymer

The cyanoacetate esters were synthesized as described elsewhere,³ with some modifications. To protect the PEG amino group during the preparation of the copolymer, we used a *t*-Boc-protected amino PEG, which allowed the synthesis of the PEG cyanoacetate by reaction of the other distal end, the hydroxyl group, with cyanoacetic acid, as shown in Scheme 1. The same procedure was followed for the synthesis of the hexadecyl cyanoacetate. Then, the cyanoacetate esters were condensed in ethanol, in the presence of formalin and dimethylamine, to form the poly(*t*-Boc-HNPEGCA-co-HDCA) copolymer. The PEG amino group was then selectively deprotected by TFA, which does not cleave ester bonds;²¹ in fact,

the composition and the MW of the copolymer were the same before and after *t*-Boc group cleavage, as found by NMR and by GPC analysis. The reaction with TFA, carried out under the conditions described, led to the cleavage of 50% of *t*-Boc groups, as found by NMR peaks integration.

Characterization of the Poly($\text{H}_2\text{NPEGCA-co-HDCA}$) Copolymer

The analysis by ^1H and ^{13}C NMR (Figures 1 and 2) confirmed the structure of the expected poly($\text{H}_2\text{NPEGCA-co-HDCA}$) copolymer. Figure 1 shows the ^1H NMR spectrum of the poly($\text{H}_2\text{NPEGCA-co-HDCA}$) copolymer: the peak at 4.26 ppm was assigned to the methylene in the α -position to the ester groups. The signal at 3.64 ppm was attributed to the PEG backbone methylene, whereas the broad peak at 2.90–2.20 ppm was assigned to the methylene protons of poly(cyanoacrylate). The peak at 1.72 ppm corresponds to the methylene in the β -position to the

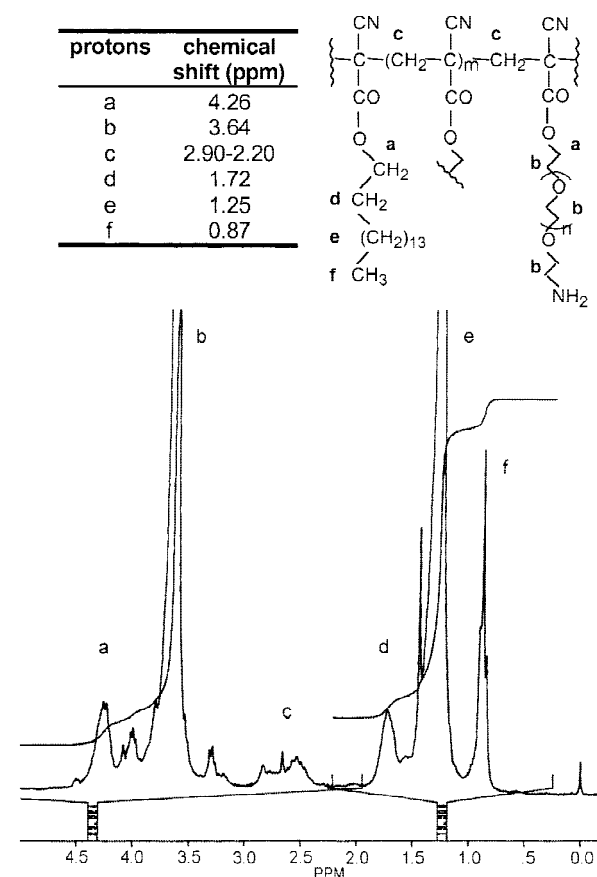


Figure 1. ^1H NMR spectrum of the poly($\text{H}_2\text{NPEGCA-co-HDCA}$) copolymer.

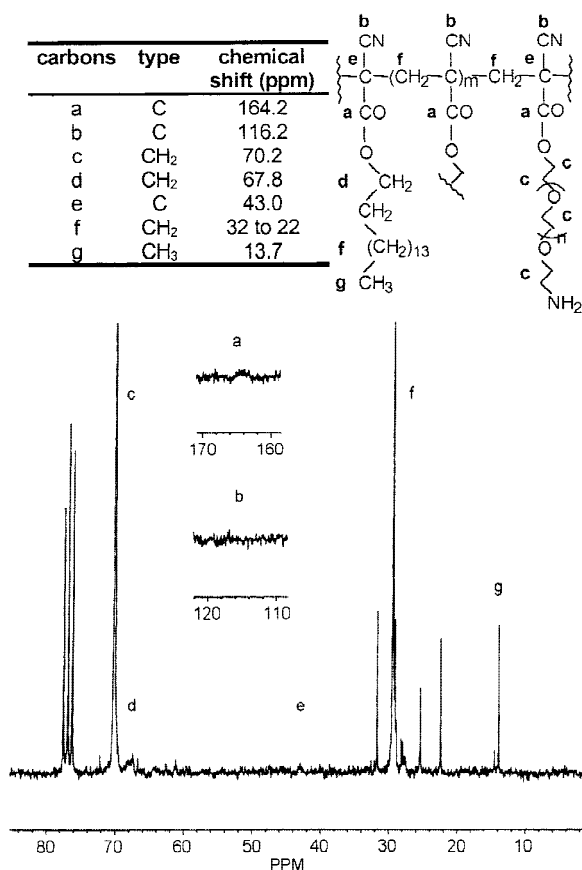


Figure 2. ^{13}C NMR spectrum of the poly($\text{H}_2\text{NPEGCA-co-HDCA}$) copolymer.

ester group of the hexadecyl chain. The singlet at 1.44 ppm was attributed to the remaining *t*-Boc groups. Finally, the peak at 1.25 ppm and the triplet at 0.87 ppm were assigned to the methylene and methyl protons of the hexadecyl chain, respectively. Moreover, the integration of the peaks corresponding to the PEG backbone and to the methylene groups of the hexadecyl chain enabled the PEG/hexadecyl chain ratio to be estimated.

As shown in Table 1, starting from a PEGCA/HDCA ratio of 1:5, the final polymer composition was 1:4.9, showing a good correlation between these two values.

Figure 2 shows the ^{13}C NMR spectrum of the poly($\text{H}_2\text{NPEGCA-co-HDCA}$) copolymer. The signals at 164.2 and 116.2 ppm were attributed to the ester carbonyl and to the cyano groups, respectively. The sharp peak at 70.2 ppm was assigned to the PEG backbone, whereas the methylene in the α -position to the ester groups showed a signal at 67.8 ppm. The peak at 43.0 ppm was

Table 1. Composition and Molecular Weight of the Poly($\text{H}_2\text{NPEGCA-co-HDCA}$)

Initial ratio PEGCA/ HDCA	Polymer composition ^a	Weight-average MW	
		Theoretical ^b	Observed ^c
1:5	1:4.9	5089	4922 \pm 400

^a Calculated from ^1H NMR spectra. ^b Calculated by considering the constitutional repeating units according to the initial ratio. ^c Calculated from GPC chromatograms.

attributed to the quaternary carbon atoms of the poly(cyanoacrylate), the hexadecyl methylene groups appear between 32 and 22 ppm, and the methyl group shows a signal at 13.7 ppm.

GPC analysis was performed to determine the mean MW and polydispersity of the poly($\text{H}_2\text{NPEGCA-co-HDCA}$) copolymer (Table 1). The average MW of the poly($\text{H}_2\text{NPEGCA-co-HDCA}$) was 4922 \pm 400 Da, with a low index of polydispersity (0.14). The MW calculated according to the initial PEGCA/HDCA ratio was 5089 Da.

Preparation and Characterization of the Nanoparticles

The nanoparticles were prepared in a single step by nanoprecipitation of PHDCA, poly(MePEGCA-co-HDCA), or poly($\text{H}_2\text{NPEGCA-co-HDCA}$). The organic solvent chosen for their preparation was acetone; nevertheless, it was necessary to heat this organic solvent because the polymers are not soluble in acetone at room temperature.

These nanoparticles showed a unimodal size distribution with a mean diameter of 96 \pm 9 nm for poly($\text{H}_2\text{NPEGCA-co-HDCA}$), 78.9 \pm 12.2 nm for the poly(MePEGCA-co-HDCA), and 89.2 \pm 26.2 nm for PHDCA nanoparticles. The size of the three types of nanoparticles was unchanged after 4 weeks at 4 $^\circ\text{C}$.

The zeta potential value of poly($\text{H}_2\text{NPEGCA-co-HDCA}$) nanoparticles was measured both in water and in 0.01 M phosphate buffer to evaluate the nanoparticles charge at different pHs and to evidence the presence of amino groups at the surface of the carrier (Table 2 and Figure 3). PHDCA and poly(MePEGCA-co-HDCA) nanoparticles were also tested as controls. It was observed that in water, the zeta potential value of noncoated PHDCA nanoparticles was lower than that of the PEG-covered ones (MePEGCA-co-HDCA and $\text{H}_2\text{NPEGCA-co-HDCA}$; Table 2). Moreover, the

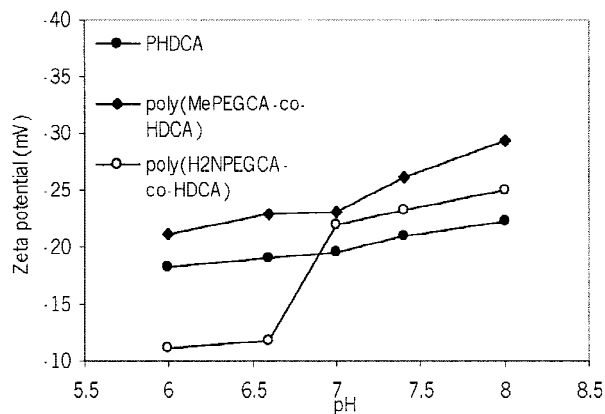
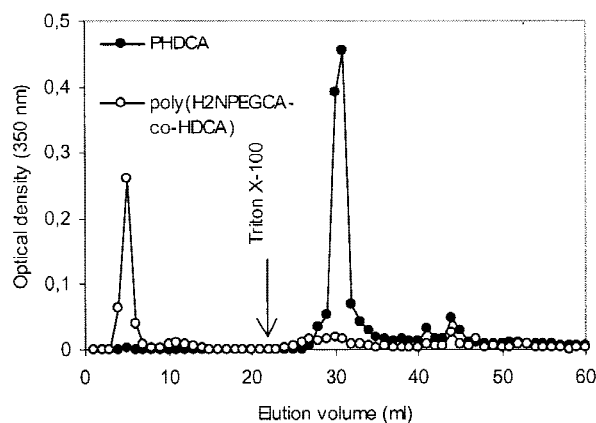
Table 2. Zeta Potential of Nanoparticles Measured in Water

Nanoparticle	Zeta potential (mV)
PHDCA	-48.06 ± 0.20
MePEG ₂₀₀₀ CA-co-HDCA	-41.13 ± 0.50
H ₂ NPEG ₃₄₀₀ CA-co-HDCA	-32.40 ± 2.10

longer PEG chains and the presence of terminal amino groups on the poly(H₂NPEGCA-co-HDCA) particles confer a less negative zeta potential value for these nanoparticles compared with the ones bearing MePEG.

In phosphate buffer with poly(H₂NPEGCA-co-HDCA) nanoparticles, a dependence of the zeta potential on the pH was observed, as shown in Figure 3. At acidic pH, there was a significant increase of the zeta potential value that corresponded to the protonation of the amino groups, whereas the zeta potential of PHDCA and poly(MePEGCA-co-HDCA) nanoparticles did not significantly change in the same range of pH. The presence of amino groups on the nanoparticles was also confirmed by the ninhydrin assay, which was positive.

HIC chromatography data (Figure 4) showed that PHDCA nanoparticles were strongly hydrophobic: they interacted with the gel phase and were removed only by washing with Triton® X-100. On the contrary, poly(H₂NPEGCA-co-HDCA) nanoparticles exhibited a more hydrophilic surface and were eluted easily.

**Figure 3.** Zeta potential-pH profiles of PHDCA, poly(MePEGCA-co-HDCA), and poly(H₂NPEGCA-co-HDCA) nanoparticles measured in 0.01 M phosphate buffer.**Figure 4.** HIC chromatograms of PHDCA and poly(H₂NPEGCA-co-HDCA) nanoparticles on a propyl agarose column eluted with PBS buffer.

Preparation and Purification of Folate-Poly(H₂NPEGCA-co-HDCA) Nanoparticles Conjugate

After poly(H₂NPEGCA-co-HDCA) nanoparticles preparation, they were covalently linked to folic acid. To activate the folate carboxylic groups for coupling with PEG terminal amino groups of the poly(H₂NPEGCA-co-HDCA) copolymer,²⁵ the NHS-ester of folic acid has been prepared, as shown in Scheme 2. Then, the NHS-folate was added to the poly(H₂NPEGCA-co-HDCA) nanoparticles suspension. The reaction of NHS-folate with PEG amino groups led to the formation of a covalent amide bond. The folic acid-nanoparticles conjugates were then purified from unreacted folic acid by Sepharose CL-4B gel chromatography, using bicarbonate buffer as eluent (Figure 5). Two distinct peaks were observed, the first one corresponding to folate-nanoparticles, which were eluted in the excluded volume, and the second one corresponding to unreacted folate. As shown in Figure 5, the separation was observed to be complete. Then, conjugated nanoparticles were dialyzed and their size was determined to verify the absence of aggregates, which could result from the coupling procedure. It was observed that the size distribution was still unimodal and the diameter near 100 nm, even if an increase in diameter was found (136 ± 47 nm instead of 96 ± 9 nm before conjugation). No change in nanoparticles size was observed after 1 month of storage (4 °C).

To investigate the surface hydrophobicity of the nanoparticles after folate conjugation, HIC chromatography analysis was performed. The folate-conjugated nanoparticles still showed a hy-

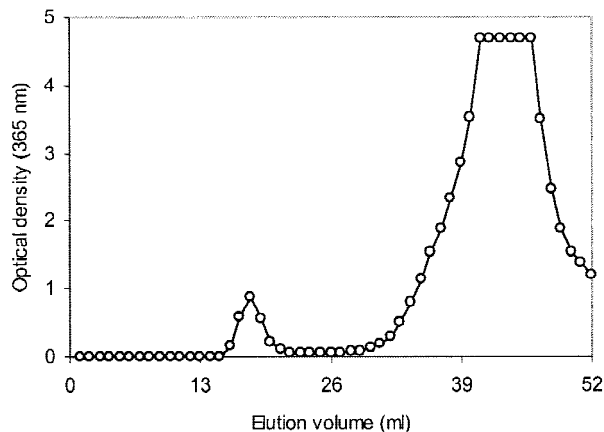


Figure 5. Gel filtration chromatogram of folate-poly($H_2NPEGCA-co-HDCA$) nanoparticles on a Sepharose CL-4B column eluted with 5 mM carbonate/bicarbonate buffer pH 9.0. UV analysis of the fractions indicated that the first peak corresponded to purified conjugated nanoparticles and the second one to the unbound folate.

drophilic surface: they did not interact with the gel phase and were eluted without the Triton® X-100; moreover, these particles were found to be in the same collected fractions of poly($H_2NPEGCA-co-HDCA$) nanoparticles before folic acid conjugation (data not shown).

Determination of Folate Content

To evaluate the extent of folate conjugation in folate-conjugated poly($H_2NPEGCA-co-HDCA$) nanoparticles, the quantitative UV analysis was performed after lyophilization of the conjugate. It was found that 14–16% of the total of PEG chains were linked to folic acid molecules.

Surface Plasmon Resonance Measurements

To evaluate the ability of folate-poly($H_2NPEGCA-co-HDCA$) nanoparticles to recognize the FBP, surface plasmon resonance analysis was performed. As shown in Figure 6A, folate-conjugated nanoparticles were able to recognize the sensorchip-immobilized FBP. On the contrary, the poly($H_2NPEGCA-co-HDCA$) nanoparticles, which were not coupled to folic acid, failed to bind onto the surface of the sensorchip in the same proportion.

To study the specificity of the interaction, binding experiments were performed in presence of 50 μM of free folic acid. As shown in Figure 6B, the amount of conjugated nanoparticles bound to the

FBP in the presence of free folic acid was just slightly lower than the one bound in the absence of free folate. Kinetic parameters for folate-nanoparticles and free folic acid are as follows: folate-conjugated nanoparticles have an apparent dissociation constant of 800 ± 170 nM (calculated from Figure 6C on the basis of 79 μM folate/2.5 mg folate-nanoparticles) and free folic acid of 11 ± 1 μM (Figure 6D).

DISCUSSION

Poly($H_2NPEGCA-co-HDCA$) copolymer was analyzed by 1H and ^{13}C NMR, which confirmed the expected structure. The GPC analysis showed a good correlation between the initial proportion of the monomers (PEGCA/HDCA, 1:5) and the measured average MW of the obtained copolymer (4922 Da measured versus 5089 Da as calculated MW theoretical value).

Nanoparticles with a size of ~ 100 nm displaying a unimodal distribution were obtained after nanoprecipitation of the poly($H_2NPEGCA-co-HDCA$) copolymer in water. It is noteworthy that using this methodology no surfactant was needed for obtaining particles in a colloidal range. This is an important point because most nanoparticle preparation methods need one or more surface-active agents to make the dispersion stable. Clearly, it is a great advantage to avoid surfactants because most of them are not allowed for intravenous administration. Now the question arises if sufficient PEG amino moieties were available at the surface of the nanoparticles for starting the folic acid coupling procedure. To answer the question, zeta potential measurements were performed in water and in phosphate buffer. The more interesting observation was that in the case of poly($H_2NPEGCA-co-HDCA$) nanoparticles, the decrease of the pH led to an increase in zeta potential value that corresponded to the protonation of the amino groups. This phenomenon was not observed with poly(MePEGCA-co-HDCA) or with non-PEGylated PHDCA nanoparticles. Such a behavior suggests that amino groups of poly($H_2NPEGCA-co-HDCA$) are well situated on the surface of the nanoparticles, letting them available for folic acid conjugation.

The presence of PEG moieties at the surface of the particles has also been evidenced by HIC chromatography, showing that poly($H_2NPEGCA-co-HDCA$) nanoparticles exhibited a more hydro-

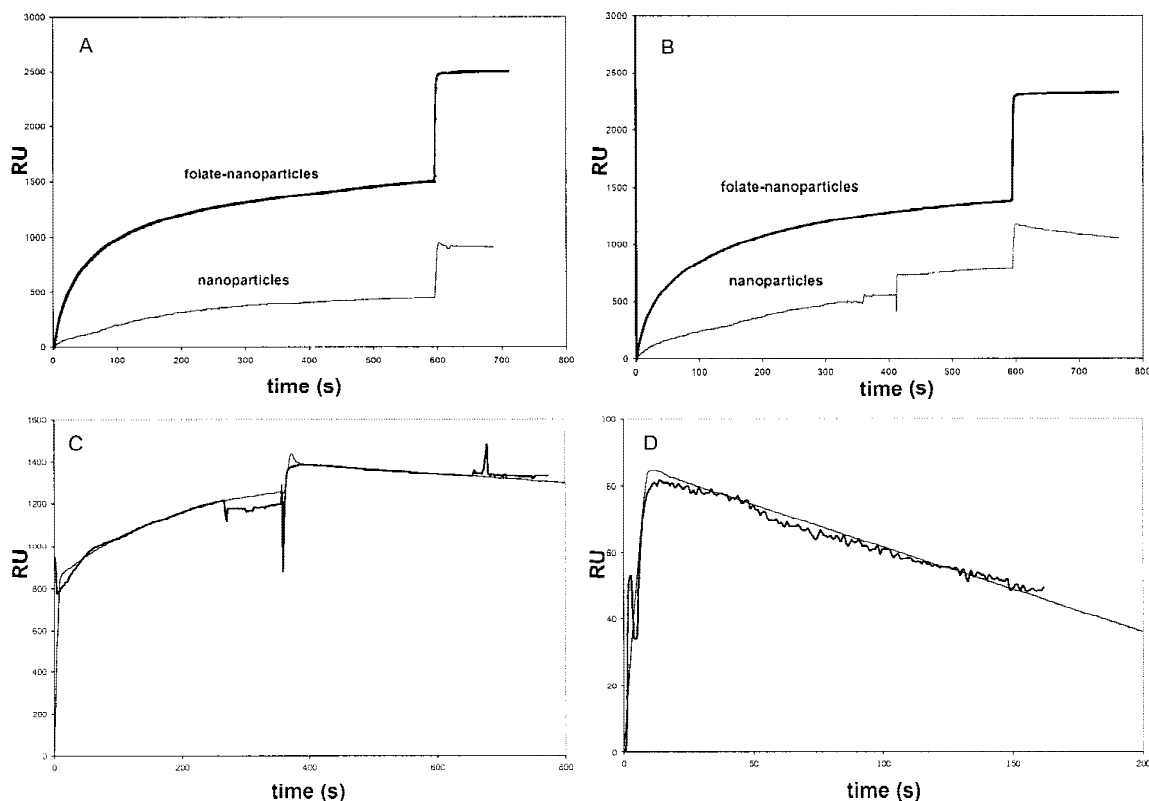


Figure 6. Surface plasmon resonance analysis of adsorption of folate-poly($H_2NPEGCA-co-HDCA$) nanoparticles on immobilized FBP. Nonconjugated poly($H_2NPEGCA-co-HDCA$) nanoparticles were used as control. These experiments were conducted according to “Experimental Section” (flow rate: $5 \mu L/min$). Every nanoparticle suspension was tested on a freshly prepared protein-covered sensor chip channel (RU = resonance units). (A) Comparison of binding of folate-nanoparticles and control nanoparticles (5 mg/mL) to FBP. (B) The same comparison in the presence of $50 \mu M$ of free folic acid. (C) Kinetic analysis of folate-nanoparticles (2.5 mg/mL corresponding to $79 \mu M$ folate) interaction with FBP. The heavy line shows the corrected sensorgram after subtraction of the sensorgram obtained with control nanoparticles. The normal line shows the theoretical curve fitting according to a two-conformation state model as calculated by BIA evaluation 3.0. The overall dissociation constant corresponds to $800 \pm 170 \text{ nM}$. (D) Kinetic analysis of folate (1 mM) interaction with FBP. As in C, the heavy line shows the sensorgram obtained for the binding of folate to FBP and the normal line shows the theoretical curve. The apparent dissociation constant was calculated as $11 \pm 1 \mu M$.

philic surface than the nonPEGylated PHDCA nanoparticles.

The reaction of activated NHS-folate with PEG terminal amino groups at the surface of poly($H_2NPEGCA-co-HDCA$) nanoparticles (Scheme 2) has then been performed to obtain a stable covalent linkage between the folic acid and the nanoparticle solid support.

This approach, which consists in the conjugation of folic acid on preformed nanoparticles, presents some advantages in respect to the coupling of folate to the copolymer before nanopar-

ticles preparation. First of all, the nanoparticles can be prepared in optimal conditions before conjugation, considering for example copolymer solubility in the organic solvents. Second, when the conjugation is performed after nanoparticles preparation, folic acid molecules may only be linked to the surface functional groups of the nanoparticles, thus being more available for folate receptor recognition. In fact, if the coupling procedure is made before nanoparticles preparation, some folate-PEG moieties can be included into the particles core and so they become unuse-

ful for folate receptor targeting. Moreover, folate-conjugated nanoparticles obtained by our procedure were very stable after 1 month of storage (4 °C).

Another step was the investigation of the surface hydrophilicity of the nanoparticles after folate conjugation. Results obtained after HIC chromatography analysis demonstrate that the conjugation of a part of the PEG moieties with folic acid does not change the surface hydrophilicity of the nanoparticles. This point is important to check because surface hydrophilicity is known to reduce the opsonization of the nanoparticles after intravenous administration, thus increasing their blood circulation time.^{2,4}

The number of PEG chains that have been conjugated to folic acid molecules has been calculated to be ~15% of total chains. To assess whether this amount of folate-PEG derivatization is sufficient to allow efficient recognition of the folate-nanoparticles by the FBP, surface plasmon resonance analysis was performed. As shown in Figure 6A, the folate-nanoparticles were able to effectively recognize the sensorchip-immobilized FBP. More remarkable was the observation that free folic acid (50 μ M) was unable to displace folate-conjugated nanoparticles from their interaction with the folate receptor (Figure 6B). Analysis of the kinetic parameters for folate-nanoparticles and free folic acid (Figure 6C and 6D) explains the low inhibitory capacity of folate as follows: folate-conjugated nanoparticles have an apparent dissociation constant of 800 ± 170 nM, calculated on the basis of 79 μ M folate/2.5 mg folate-nanoparticles. This affinity is due to two binding steps: a fast one comparable to that of free folate and a slow isomerization step (Figure 6C). In contrast, folic acid has an apparent dissociation constant of only 11 ± 1 μ M (Figure 6D), necessitating thus at least a 108-fold higher molar concentration over 79 μ M to completely inhibit the interaction of folate-nanoparticles with FBP. This concentration is over the solubility limit of folic acid under the experimental conditions. The greater binding avidity of folate-conjugated nanoparticles towards FBP may be explained as follows: these particles represent a multivalent form of the ligand folic acid, and folate receptors are often disposed in clusters; thus, conjugated nanoparticles could display a multivalent stronger interaction with FBP. For this reason, the slow isomerization step is supposed to correspond to the clustering of FBP on the chip (Figure 7).

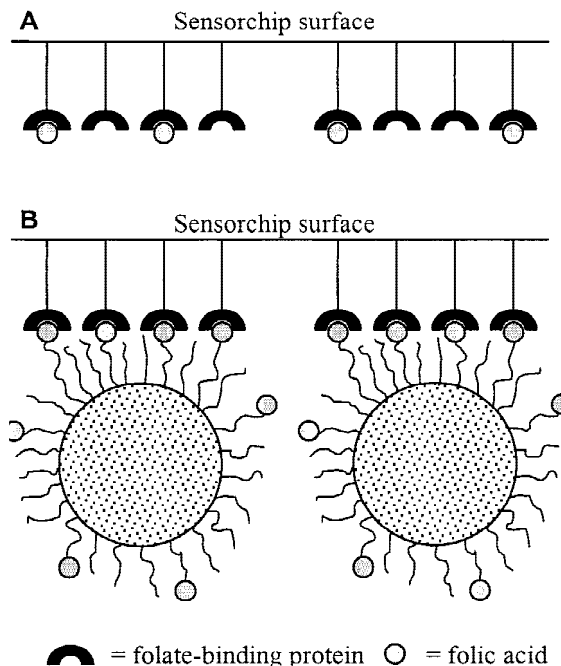


Figure 7. Schematic representation of the interaction of free folic acid and folate-conjugated nanoparticles with the immobilized FBP. (A) Free folic acid has a single interaction with the receptor. (B) Folate-conjugated nanoparticles display a multivalent interaction with the clusters of the FBP.

The relative low affinities measured in the BI-Acore system compared with the known affinities for folate of the FBP could be explained in two ways. Immobilization of the binding protein could alter its properties by linking the free lysine residues in an amide bond to the carboxylated dextran. Alternatively, immobilization could inhibit the conformational changes, which are leading to high affinity binding. Whatever the mechanism, the fact remains that folate bound to nanoparticles has a 10-fold higher apparent affinity for the FBP than free folate.

Thus, the prepared nanoparticles represent a new potential delivery system for compounds with anticancer activity because folate receptor is frequently overexpressed onto the surface of malignant cells. Moreover, the encapsulation of anticancer drugs into folate-conjugated nanoparticles could not only increase the specific drug delivery towards target tumoral cells, but it may also present the advantages to protect the drug from *in vivo* degradation (case of antisense oligonucleotides, for example) and to reduce drug side effects and toxicity.

CONCLUSIONS

In this study we have synthesized and characterized a novel amphiphilic PEG cyanoacrylate copolymer with terminal amino groups. This copolymer allowed the preparation of stable and small-sized nanoparticles, which were found to be an excellent solid support for coupling activated folic acid. The analysis by surface plasmon resonance showed that the folate-nanoparticles conjugates were able to bind specifically to the immobilized FBP, whereas nanoparticles without folic acid targeting moieties showed a much lower interaction.

In conclusion, these PEGylated and targeted nanoparticles represent potential carriers for tumor cell-selective targeting of antitumoral drugs. Further studies are in progress to test this new drug delivery system *in vivo*.

ACKNOWLEDGMENTS

This work was supported by MURST 60–40% (Progetto Nazionale “Tecnologie Farmaceutiche”) and by CNRS (programme “Physique et Chimie du Vivant”) grants.

REFERENCES

1. Stolnik S, Illum L, Davis SS. 1995. Long circulating microparticulate drug carriers. *Adv Drug Del Rev* 16:195–214.
2. Gref R, Minamitake Y, Peracchia MT, Langer R. 1996. PEG-coated biodegradable nanospheres for intravenous drug administration. In Cohen S, Bernstein H, editors. *Microparticulate systems for the delivery of proteins and vaccines*, New York: Marcel Dekker, pp 279–306.
3. Peracchia MT, Desmaële D, Couvreur P, d'Angelo J. 1997. Synthesis of a novel poly(MePEG cyanoacrylate-co-alkyl cyanoacrylate) amphiphilic copolymer for nanoparticle technology. *Macromolecules* 30:846–851.
4. Peracchia MT, Fattal E, Desmaële D, Besnard M, Noël JP, Gomis JM, Appel M, d'Angelo J, Couvreur P. 1999. Stealth® PEGylated polycyanoacrylate nanoparticles for intravenous administration and splenic targeting. *J Controlled Release* 60:121–128.
5. Blume G, Cevc G, Crommelin MDJA, Bakker-Woudenberg IAJM, Kluft C, Storm G. 1993. Specific targeting with poly(ethylene glycol)-modified liposomes: Coupling of homing devices to the ends of the polymeric chains combines effective target binding with long circulation times. *Biochim Biophys Acta* 1149:180–184.
6. Kaplan MR, Calef E, Bercovici T, Gitler C. 1983. The selective detection of cell surface determinants by means of antibodies and acetylated avidin attached to highly fluorescent polymer microspheres. *Biochim Biophys Acta* 728:112–120.
7. Kumakura M, Suzuki M, Adachi S, Kaetsu I. 1983. Polyacrolein microspheres as immunoreagents. *J Immunol Methods* 63:115–122.
8. Bourel D, Rolland A, Le Verge R, Genetet B. 1988. CD3 monoclonal antibody covalently coupled to fluorescent polymethacrylic nanoparticles. *J Immunol Methods* 106:161–167.
9. Franklin WA, Waintrub M, Edwards D, Christensen K, Prendegast P, Woods J, Bunn PA, Kolhouse JF. 1994. New anti-lung cancer antibody cluster 12 reacts with human folate receptors present on adenocarcinoma. *Int J Cancer Suppl* 8: 89–95.
10. Weitman SD, Lark RH, Coney LR, Fort DW, Frasca V, Zurawski VR, Kamen BA. 1992. Distribution of the folate receptor GP38 in normal and malignant cell lines and tissues. *Cancer Res* 52:3396–3401.
11. Coney LR, Tomassetti A, Carayannopoulos L, Frasca V, Kamen BA, Colnaghi MI, Zurawski WR. 1991. Cloning of a tumor-associated antigen: Mov18 and Mov19 antibodies recognize a folate-binding protein. *Cancer Res* 51:6125–6132.
12. Garin-Chesa P, Campbell I, Saigo PE, Lewis JL, Old LJ, Rettig WJ. 1993. Trophoblast and ovarian cancer antigen LK26. Sensitivity and specificity in immunopathology and molecular identification as a folate-binding protein. *Am J Pathol* 142:557–567.
13. Campbell IG, Jones TA, Foulkes WD, Trowsdale J. 1991. Folate-binding protein is a marker for ovarian cancer. *Cancer Res* 51:5329–5338.
14. Antony AC. 1992. The biological chemistry of folate receptors. *Blood* 79:2807–2820.
15. Rothberg KG, Ying YS, Kolhouse JF, Kamen BA, Anderson RG. 1990. The glycopospholipid-linked folate receptor internalizes folate without entering the clathrin-coated pit endocytic pathway. *J Cell Biol* 110:637–649.
16. Wang S, Lee RJ, Mathias CJ, Green MA, Low PS. 1996. Synthesis, purification, and tumor cell uptake of Gallium-67-deferoxamine-folate, a potential radiopharmaceutical for tumor imaging. *Bioconjugate Chem* 7:56–62.
17. Lee RJ, Low PS. 1994. Delivery of liposomes into cultured KB cells via folate receptor-mediated endocytosis. *J Biol Chem* 269:3198–3204.
18. Wang S, Low PS. 1998. Folate-mediated targeting of antineoplastic drugs, imaging agents, and nucleic acids to cancer cells. *J Controlled Release* 53:39–48.
19. Gabizon A, Horowitz AT, Goren D, Tzemach D, Mandelbaum-Shavit F, Qazen MM, Zalipsky S.

1999. Targeting folate receptor with folate linked to extremities of poly(ethylene glycol)-grafted liposomes: in vitro studies. *Bioconjugate Chem* 10: 289–298.
20. Malmqvist M. 1993. Biospecific interaction analysis using biosensor technology. *Nature* 361:186–187.
21. Tarbell DS, Yamamoto Y, Pope BM. 1972. New method to prepare N-t-butoxycarbonyl derivatives and the corresponding sulfur analogs from di-t-butyl dicarbonate or di-t-butyl dithiol dicarbonates and amino acids. *Proc Nat Acad Sci, USA* 69:730–732.
22. Fessi H, Puisieux F, Devissaguet JPh, Ammoury N, Benita S. 1989. Nanocapsule formation by interfacial polymer deposition following solvent displacement. *Int J Pharm* 55:R1–R4.
23. Löfås S, Johnsson B. 1990. A novel hydrogel matrix on gold surfaces plasmon resonance sensors for fast and efficient covalent immobilisation of ligands. *J Chem Soc Chem Commun* 21:1526–1528.
24. Johnsson B, Löfås S, Lindquist G. 1991. Immobilization of proteins to a carboxymethyl-dextran-modified gold surface for biospecific interaction analysis in surface plasmon resonance sensors. *Anal Biochem* 198:268–277.
25. Mattson G, Conklin E, Desai S, Nielander G, Savage MD, Morgensen S. 1993. A practical approach to crosslinking. *Mol Biol Rep* 17:167–183.